# Analysis of residual stresses generated by progressive induction hardening of steel cylinders

**P M C L Pacheco**[1]*, **M A Savi**[2] and **A F Camarão**[3]
[1]Department of Mechanical Engineering, CEFET/RJ, Rio de Janeiro, Brazil
[2]Department of Mechanical and Materials Engineering, Instituto Militar de Engenharia, Rio de Janeiro, Brazil
[3]Debis Humaitá IT, Services Latin America Ltda, São Paulo, Brazil

**Abstract:** The internal stresses generated during quenching can produce warping and even cracking of a steel body and, therefore, the prediction of such stresses is an important task. Phenomenological aspects of quenching involve couplings between different physical processes occurring in the phenomena. The present contribution is concerned with modelling and simulation of quenching, presenting an anisothermal model formulated within the framework of continuum mechanics and the thermodynamics of irreversible processes. A numerical procedure is developed based on an operator split technique associated with an iterative numerical scheme in order to deal with non-linearities in the formulation. With this assumption, the coupled governing equations are solved involving four uncoupled problems: thermal, phase transformation, thermoelastic and elastoplastic behaviours. The proposed general formulation is applied to analyse progressive induction hardening of steel cylinders. Numerical results suggest that the proposed model is capable of capturing the main behaviour observed in experimental data.

**Keywords:** quenching, phase transformation, numerical simulation, modelling

## NOTATION

| | |
|---|---|
| $a_\mathrm{I}$ | internal coupling term |
| $a_\mathrm{T}$ | thermal coupling term |
| $c$ | specific heat $= -(T/\rho)\,(\partial^2 W/\partial T^2)$ |
| $C_1$, $C_2$ | positive constants |
| $d_1$ | mechanical dissipation |
| $d_2$ | thermal dissipation |
| $E$ | Young's modulus |
| $E_{ijkl}$ | elastic tensor |
| $g_i$ | $= (1/T)\,(\partial T/\partial x_i)$ |
| $H$ | material parameter associated with kinematic hardening |
| $H_{ijkl}$ | hardening tensor |
| $I_\beta(\beta)$ | indicator function associated with convex $C_\beta = \{\beta \mid 0 \leqslant \beta \leqslant 1\}$ |
| $I_f^*(P_{ij}, X_{ij})$ | indicator function associated with elastic domain |
| $k$ | material constant |
| $M_\mathrm{f}$ | temperature where martensite finishes its formation in the stress-free state |
| $M_\mathrm{s}$ | temperature where martensite starts to form in the stress-free state |
| $P_{ij}^\mathrm{d}$ | $= \sigma_{ij}^\mathrm{d}$ |
| $q_i$ | heat flux vector |
| $r, \theta, z$ | cylindrical coordinates |
| $R$ | cylinder radius |
| $T$ | temperature |
| $T_0$ | reference temperature |
| $u$ | radial displacement |
| $W$ | energy function |
| $X_{ij}^\mathrm{d}$ | $= X_{ij} - \delta_{ij}(X_{kk}/3)$ |
| $\alpha_{ij}$ | variable related to kinematic hardening |
| $\alpha_\mathrm{T}$ | coefficient of linear thermal expansion |
| $\beta$ | volumetric fraction of martensitic phase |
| $\gamma$ | material property related to the total expansion associated with martensitic transformation |
| $\delta_{ij}$ | Kronecker delta |
| $\varepsilon_{ij}$ | total strain tensor |
| $\varepsilon_{ij}^\mathrm{e}$ | elastic strain tensor |
| $\varepsilon_{ij}^\mathrm{p}$ | plastic strain tensor |
| $\varepsilon_{ij}^\mathrm{tp}$ | transformation plasticity strain tensor |
| $\varepsilon_{ij}^\mathrm{tv}$ | volumetric strain tensor |
| $\varepsilon_{ij}^\mathrm{T}$ | thermal strain tensor |
| $\zeta(T, \dot{T})$ | function associated with phase transformation kinetics |
| $\kappa$ | material parameter |
| $\lambda$ | plastic multiplier |
| $\Lambda$ | coefficient of thermal conductivity |

*The MS was received on 9 January 2001 and was accepted after revision for publication on 18 May 2001.*
**Corresponding author: Department of Mechanical Engineering, CEFET/RJ, Av. Maracana 229, 20271-110 Rio de Janeiro, RJ, Brazil.*

| | |
|---|---|
| $\nu$ | Poisson's ratio |
| $\rho$ | material density |
| $\sigma_{ij}$ | stress tensor component |
| $\sigma_{ij}$, $P_{ij}$, $Q_{ij}$, $R_{ij}$, $X_{ij}$, $Z$, $s$ | thermodynamic forces associated with state variables |
| $\sigma_{ij}^{\mathrm{d}}$ | deviatoric stress component $= \sigma_{ij} - \delta_{ij}(\sigma_{kk}/3)$ |
| $\sigma_{\mathrm{Y}}$ | material yield stress |
| $\omega$, $\omega^*$ | pseudo-potential of dissipation and its dual |
| $\chi$ | heat conversion factor |
| $\psi$ | Helmholtz free energy |
| | |
| $\partial()$ | subdifferential of the ( ) |
| $()_i$ with $i = r, \theta, z$ | normal components of the second-order tensors in cylindrical coordinates |

## 1 INTRODUCTION

Quenching is a commonly used heat treatment to increase the strength of steels by the formation of a hard microstructure called martensite. In brief, quenching consists of raising the temperature of the steel above a certain critical temperature, called the austenitizing temperature, holding it at that temperature for a fixed time and then rapidly cooling it in a suitable medium to room temperature. The resulting microstructures formed from quenching (pearlite, bainite and martensite) depend on the cooling rate and on the steel characteristics expressed by the isothermal transformation (IT) diagram. If the steel is cooled sufficiently rapidly following austenitizing, the formation of pearlite and bainite is avoided, and martensite is produced. $M_{\mathrm{s}}$ is the temperature where martensite starts to form in the stress-free state, and the formation of martensite finishes at $M_{\mathrm{f}}$. In order to avoid austenite decomposition before $M_{\mathrm{s}}$ is reached, achieving a totally martensitic microstructure, alloying elements are added to steels to modify the IT curves. The volumetric expansion associated with the formation of martensite combined with large temperature gradients and non-uniform cooling promote high residual stresses in quenched steels. The prediction of such stresses is a rather difficult task.

Phenomenological aspects of quenching involve couplings between different physical processes and, therefore, its description is unusually complex. Basically, three couplings are essential [**1**–**5**]:

1. *Thermal phenomena.* Heat transfer causes temperature variations that change the physical properties of the material.
2. *Phase transformation.* Two types of modification occur when phase transformation takes place. The first type is a kinetic modification and sometimes leads to a different morphology in the phase produced. The second type, on the other hand, is a mechanical modification related to the progress of transformation and it takes place when plastic deformation occurs under stresses lower than the yield stress of the material [**1**].
3. *Mechanical aspects.* Temperature evolution and phase transformations cause elastic and plastic deformations, resulting in residual stresses.

Usually, quenching represents one of the last stages in the fabrication of mechanical components. Since the process may induce distortion or even cracking, it is important to predict the residual stresses caused by this process. Many studies have been devoted to this aim [**1**–**5**]; however, the proposed models are not generic and are usually applicable only to simple geometries.

Progressive induction hardening applied to bodies previously quenched and tempered is a heat treatment process carried out by moving a workpiece at a constant speed through a coil and a cooling ring. Applying an a.c. to the coil, a magnetic field is generated which induces eddy currents in the workpiece and through the eddy current losses it becomes heated. During heating, a thin surface layer of austenite is formed. During subsequent quenching, this layer is transformed into martensite, pearlite, bainite and proeutectoid ferrite–cementite depending on, among other things, the cooling rate. A hard surface layer with high compressive residual stresses, combined with a tough core with tensile residual stresses, is often obtained.

The present contribution is concerned with modelling and simulation of the quenching process. An anisothermal model formulated within the framework of continuum mechanics and the thermodynamics of irreversible processes is presented [**6**, **7**]. Therefore, it is possible to identify couplings, estimating the effect of each on the process. A numerical procedure is developed based on the operator split technique [**8**] associated with an iterative numerical scheme in order to deal with non-linearities in the formulation. With this assumption, the coupled governing equations are solved from four uncoupled problems: thermal, phase transformation, thermoelastic and elastoplastic. The proposed general formulation is applied to the progressive induction hardening of steel cylinders. Numerical results suggest that the proposed model is capable of capturing the main behaviour observed on experimental data.

## 2 PHENOMENOLOGICAL ASPECTS OF PHASE TRANSFORMATION

Deformation of the material during the phase transformation process from austenite to martensite results from interactions of many phenomena. It is postulated here that the total strain increment $\mathrm{d}\varepsilon_{ij}$, can be divided into five parts [**4**]:

$$\mathrm{d}\varepsilon_{ij} = \mathrm{d}\varepsilon_{ij}^{\mathrm{e}} + \mathrm{d}\varepsilon_{ij}^{\mathrm{T}} + \mathrm{d}\varepsilon_{ij}^{\mathrm{p}} + \mathrm{d}\varepsilon_{ij}^{\mathrm{tv}} + \mathrm{d}\varepsilon_{ij}^{\mathrm{tp}} \qquad (1)$$

Here the index notation is used employing summation convention where repeated indices imply summing over the range of the index (1, 2, 3) [**6**]; $d\varepsilon_{ij}^{e}$, $d\varepsilon_{ij}^{T}$ and $d\varepsilon_{ij}^{p}$ are increments of elastic, thermal and plastic strains respectively [**7**]. Also, $d\varepsilon_{ij}^{tv}$ and $d\varepsilon_{ij}^{tp}$ are associated with phase transformation processes denoting the volumetric and the transformation plasticity components respectively.

Phase transformation from austenite to martensite is accompanied by a volumetric expansion, which usually is near 4 per cent. Therefore, when part of a material experiences phase transformation, there is an increment of volumetric deformation, $d\varepsilon_{ij}^{tv}$, given by [**1**]

$$d\varepsilon_{ij}^{tv} = \gamma \, d\beta \, \delta_{ij} \tag{2}$$

where $d\beta$ is the increment of volumetric fraction of martensitic phase formed during the decrease in temperature, $\gamma$ is a material property related to the total expansion associated with martensitic transformation and $\delta_{ij}$ is the Kronecker delta [**6**].

The increment of transformation plasticity deformation, $d\varepsilon_{ij}^{tp}$, is the result of several physical mechanisms. The development of a model for material behaviour may be based on phenomenological aspects where the martensitic transformation causes localized plastic deformation. Many researchers agree with the following expression to describe the phenomenon [**1**, **4**, **9**]:

$$d\varepsilon_{ij}^{tp} = 3\kappa\sigma_{ij}^{d}(1-\beta)\, d\beta \tag{3}$$

where $\kappa$ is a material parameter, $\sigma_{ij}^{d} = \sigma_{ij} - \delta_{ij}(\sigma_{kk}/3)$ is the deviatoric stress component and $\sigma_{ij}$ is the stress tensor component. It should be emphasized that this deformation may be related to stress states that are inside the yield surface.

The kinetics of phase transformation from austenite to martensite may be expressed by the equation proposed by Koistinen and Marburger [**10**]:

$$\beta = 1 - \exp[-k(M_s - T)] \tag{4}$$

where $k$ is a material constant, $T$ is the temperature and $M_s$ is the temperature where martensite starts to form under stress-free state. It is also convenient to define the temperature where martensite finishes its formation, estimating the asymptotic value of the exponential law (4): $M_f = M_s - [2\log(10)]/k$.

## 3 CONSTITUTIVE MODEL

The thermodynamic state of a solid is completely defined by knowledge of the state variables. Constitutive equations may be formulated within the framework of continuum mechanics and the thermodynamics of irreversible processes, by considering thermodynamic forces, defined from the Helmholtz free energy $\psi$ and thermodynamic fluxes, defined from the pseudo-potential of dissipation $\omega$ [**7**].

The quenching model proposed here allows different coupling phenomena to be identified, estimating the effect of each in the process. With this aim, a Helmholtz free energy is proposed as a function of observable variables, total deformation $\varepsilon_{ij}$ and temperature $T$. Also, internal variables are considered: plastic deformation $\varepsilon_{ij}^{p}$, volumetric fraction of martensitic phase $\beta$, and another set of variables associated with the phase transformation, hardening and damage effects. Here, this set considers a variable related to kinematic hardening, $\alpha_{ij}$, and two variables related to the martensitic phase transformation: volumetric strain tensor $\varepsilon_{ij}^{tv}$ and transformation plasticity strain tensor $\varepsilon_{ij}^{tp}$. Therefore, the following free energy is considered:

$$\rho\psi(\varepsilon_{ij}^{e}, \alpha_{ij}, \beta, T) = W(\varepsilon_{ij}^{e}, \alpha_{ij}, \beta, T)$$
$$= W_e(\varepsilon_{ij}^{e}) + W_\alpha(\alpha_{ij}) + W_\beta(\beta) - W_T(T) \tag{5}$$

where $\varepsilon_{ij}^{e} = \varepsilon_{ij} - \alpha_T(T - T_0)\delta_{ij} - \varepsilon_{ij}^{p} - \varepsilon_{ij}^{tv} - \varepsilon_{ij}^{tp}$ is the elastic deformation and the energy functions are given by the following expressions:

$$W_e = \tfrac{1}{2}E_{ijkl}\varepsilon_{ij}^{e}\varepsilon_{kl}^{e}$$

$$W_\alpha(\alpha_{ij}) = \tfrac{1}{2}H_{ijkl}\alpha_{ij}\alpha_{kl}$$

$$W_\beta(\beta) = I_\beta$$

$$W_T(T) = \rho\int_{T_0}^{T} C_1 \log(\xi)\, d\xi + \frac{\rho}{2}C_2T^2 \tag{6}$$

The components $E_{ijkl}$ and $H_{ijkl}$ are associated with elastic and hardening tensors and $\alpha_T$ is the coefficient of linear thermal expansion. These parameters are temperature dependent; $C_1$ and $C_2$ are positive constants, $T_0$ is a reference temperature and $\rho$ is the material density; $I_\beta(\beta)$ is the indicator function associated with convex $C_\beta = \{\beta | 0 \leqslant \beta \leqslant 1\}$ [**11**].

The thermodynamic forces ($\sigma_{ij}$, $P_{ij}$, $Q_{ij}$, $R_{ij}$, $X_{ij}$, $Z$, $s$), associated with the state variables ($\varepsilon_{ij}$, $\varepsilon_{ij}^{p}$, $\varepsilon_{ij}^{tv}$, $\varepsilon_{ij}^{tp}$, $\alpha_{ij}$, $\beta$, $T$), are defined from $W$, as follows [**7**]:

$$\sigma_{ij} = \frac{\partial W}{\partial \varepsilon_{ij}} = E_{ijkl}\varepsilon_{kl}^{e} \tag{7}$$

$$P_{ij} = -\frac{\partial W}{\partial \varepsilon_{ij}^{p}} = \sigma_{ij} \tag{8}$$

$$Q_{ij} = -\frac{\partial W}{\partial \varepsilon_{ij}^{tv}} = \sigma_{ij} \tag{9}$$

$$R_{ij} = -\frac{\partial W}{\partial \varepsilon_{ij}^{tp}} = \sigma_{ij} \tag{10}$$

$$X_{ij} = \frac{\partial W}{\partial \alpha_{ij}} = H_{ijkl}\alpha_{kl} \tag{11}$$

$$Z \in \partial_\beta I_\beta(\beta) \tag{12}$$

$$s = -\frac{1}{\rho}\frac{\partial W}{\partial T} \tag{13}$$

where $\partial_\beta I_\beta(\beta)$ is the subdifferential of the indicator function $I_\beta$ [11].

In order to describe dissipation processes, it is necessary to introduce a potential of dissipation, $\omega(\dot{\varepsilon}^{p}_{ij}, \dot{\varepsilon}^{tv}_{ij}, \dot{\varepsilon}^{tp}_{ij}, \dot{\alpha}_{ij}, \dot{\beta}, q_i)$, which can be split into two parts: $\omega(\dot{\varepsilon}^{p}_{ij}, \dot{\varepsilon}^{tv}_{ij}, \dot{\varepsilon}^{tp}_{ij}, \dot{\alpha}_{ij}, \dot{\beta}, q_i) = \omega_1(\dot{\varepsilon}^{p}_{ij}, \dot{\varepsilon}^{tv}_{ij}, \dot{\varepsilon}^{tp}_{ij}, \dot{\alpha}_{ij}, \dot{\beta}) + \omega_2(q_i)$. Also, this potential can be written through its dual $\omega^*(P_{ij}, Q_{ij}, R_{ij}, X_{ij}, Z, g_i) = \omega_1^*(P_{ij}, Q_{ij}, R_{ij}, X_{ij}, Z) + \omega_2^*(g_i)$, as follows:

$$\omega_1^* = I_f^*(P_{ij}, X_{ij}) + \gamma\dot{\beta}Q_{ij} + \frac{3\kappa\dot{\beta}(1-\beta)}{2}\left(R_{ij} - \frac{R_{kk}}{3}\delta_{ij}\right) \times \left(R_{ij} - \frac{R_{kk}}{3}\delta_{ij}\right) + \zeta(T, \dot{T})Z$$

$$\omega_2^* = \frac{T}{2}\Lambda g_i g_i \tag{14}$$

where $\zeta(T, \dot{T})$ is a function associated with phase transformation kinetics, $g_i = (1/T)(\partial T/\partial x_i)$ and $\Lambda$ is the coefficient of thermal conductivity which is function of temperature; $I_f^*(P_{ij}, X_{ij})$ is the indicator function associated with elastic domain, related to the von Mises criterion:

$$f(P_{ij}, X_{ij}) = [\tfrac{3}{2}(P^{d}_{ij} - X^{d}_{ij})(P^{d}_{ij} - X^{d}_{ij})]^{1/2} - \sigma_Y \leqslant 0 \tag{15}$$

$\sigma_Y$ is the material yield stress, $X^{d}_{ij} = X_{ij} - \delta_{ij}(X_{kk}/3)$ and $P^{d}_{ij} = \sigma^{d}_{ij}$. A set of evolution laws obtained from $\omega^*$ characterizes dissipative processes:

$$\dot{\varepsilon}^{p}_{ij} \in \partial_{P_{ij}} I_f^*(P_{ij}, X_{ij}) = \lambda\,\mathrm{sgn}(\sigma_{ij} - H_{ijkl}\alpha_{kl}) \tag{16}$$

$$\dot{\varepsilon}^{tv}_{ij} = \frac{\partial\omega^*}{\partial Q_{ij}} = \gamma\dot{\beta}\delta_{ij} \tag{17}$$

$$\dot{\varepsilon}^{tp}_{ij} = \frac{\partial\omega^*}{\partial R_{ij}} = 3\kappa\dot{\beta}(1-\beta)\sigma^{d}_{ij} \tag{18}$$

$$\dot{\alpha}_{ij} \in -\partial_{X_{ij}} I_f^*(\sigma_{ij}, X_{ij}) = \dot{\varepsilon}^{p}_{ij} \tag{19}$$

$$\dot{\beta} = -\frac{\partial\omega^*}{\partial Z} = -\zeta(T,\dot{T}) \tag{20}$$

$$q_i = -\frac{\partial\omega^*}{\partial g_i} = -\Lambda T g_i = -\Lambda\frac{\partial T}{\partial x_i} \tag{21}$$

where $\mathrm{sgn}(x) = x/|x|$, $q_i$ is the heat flux vector, $\lambda$ is the plastic multiplier from the classical theory of plasticity [7] and $\zeta(T, \dot{T})$ is defined by the following equation:

$$\zeta(T, \dot{T}) = \begin{cases} k\dot{T}\exp[-k(M_s - T)] & \text{if } M_s \geqslant T \geqslant M_f \\ 0 & \text{if } T > M_s \text{ and } T < M_f \end{cases} \tag{22}$$

Using the following definition for the specific heat $c = -(T/\rho)(\partial^2 W/\partial T^2)$ and the set of constitutive equations (7) to (13) and (16) to (21), the heat equation can be written as

$$\frac{\partial}{\partial x_i}\left(\Lambda\frac{\partial T}{\partial x_i}\right) - \rho c\dot{T} = -a_I - a_T \tag{23}$$

where

$$a_I = \sigma_{ij}(\dot{\varepsilon}^{p}_{ij} + \dot{\varepsilon}^{tv}_{ij} + \dot{\varepsilon}^{tp}_{ij}) - X_{ij}\dot{\alpha}_{ij} - Z\dot{\beta}$$

$$a_T = T\left(\frac{\partial\sigma_{ij}}{\partial T}\dot{\varepsilon}^{e}_{ij} + \frac{\partial X_{ij}}{\partial T}\dot{\alpha}_{ij} + \frac{\partial Z}{\partial T}\dot{\beta}\right) \tag{24}$$

The term $a_I$ is denoted as internal coupling and is always positive. It has a role in equation (23) similar to a heat source in the classical heat equation for rigid bodies. The term $a_T$ denotes the thermal coupling and can be either positive or negative.

With these assumptions, the set of constitutive equations formed by equations (7) to (13) and (16) to (21) verify the inequality established by the second law of thermodynamics which can be expanded in a local form as

$$d_1 = \sigma_{ij}(\dot{\varepsilon}^{p}_{ij} + \dot{\varepsilon}^{tv}_{ij} + \dot{\varepsilon}^{tp}_{ij}) - X_{ij}\dot{\alpha}_{ij} - Z\dot{\beta} \geqslant 0$$

$$d_2 = -(q_i g_i) \geqslant 0 \tag{25}$$

The term $d_1$ represents mechanical dissipation while $d_2$ is thermal dissipation.

In metal forming, the thermomechanical coupling is usually taken into account by an empirical constant called the heat conversion factor, which represents the part of the plastic power transformed into heat [12]:

$$\chi = \frac{a_I + a_T}{\sigma_{ij}\dot{\varepsilon}^{p}_{ij}} \tag{26}$$

## 4 CYLINDRICAL BODIES

This contribution considers cylindrical bodies as an application of the proposed general formulation. Other researchers have presented different analyses of this problem [**13**, **14**]. With this assumption, heat transfer analysis may be reduced to a one-dimensional problem. Also, a plane stress or plane strain state can be assumed. Under these assumptions, only radial $r$, tangential $\theta$ and longitudinal $z$ components need to be considered and a one-dimensional model is formulated. In order to present simplified equations, the normal components of the second-order tensors ($\varepsilon_{ij}$, $\sigma_{ij}$, $\alpha_{ij}$, for $i = j$) are denoted by $(\,)_i$ with $i = r, \theta, z$ and the summation convention is not evoked.

At first, consider the isotropic Hooke law to establish a relation between stresses and elastic strains [**15**]:

$$\varepsilon_r^{\mathrm{e}} = \frac{1}{E}[\sigma_r - \nu(\sigma_\theta + \sigma_z)] \tag{27}$$

$$\varepsilon_\theta^{\mathrm{e}} = \frac{1}{E}[\sigma_\theta - \nu(\sigma_r + \sigma_z)] \tag{28}$$

$$\varepsilon_z^{\mathrm{e}} = \frac{1}{E}[\sigma_z - \nu(\sigma_r + \sigma_\theta)] \tag{29}$$

where $E$ and $\nu$ are Young's modulus and Poisson's ratio respectively. The thermal strain is defined as

$$\varepsilon_i^{\mathrm{T}} = \alpha_{\mathrm{T}}(T - T_0), \qquad \text{for } i = r, \theta, z \tag{30}$$

The evolution equations for plastic variables are described by

$$\dot{\varepsilon}_i^{\mathrm{p}} = \lambda\,\mathrm{sgn}(\sigma_i - H\alpha_i), \qquad \text{for } i = r, \theta, z \tag{31}$$

where $H$ is a material parameter associated with kinematic hardening [**7**, **16**]. The yield function, associated with the elastic domain, is defined by employing the von Mises criteria:

$$\sqrt{\tfrac{1}{2}[(\sigma_r^* - \sigma_z^*)^2 + (\sigma_r^* - \sigma_\theta^*)^2 + (\sigma_\theta^* - \sigma_z^*)^2]} - \sigma_{\mathrm{Y}} \leqslant 0 \tag{32}$$

with the following definitions:

$$\sigma_i^* = \sigma_i^{\mathrm{d}} - H\alpha_i^{\mathrm{d}}$$

$$\sigma_i^{\mathrm{d}} = \sigma_i - \frac{\sigma_r + \sigma_\theta + \sigma_z}{3}$$

$$\alpha_i^{\mathrm{d}} = \alpha_i - \frac{\alpha_r + \alpha_\theta + \alpha_z}{3}$$

$$\text{for } i = r, \theta, z \tag{33}$$

The evolution equations for the deformation related to martensitic phase transformation are described by

$$\dot{\varepsilon}_i^{\mathrm{tv}} = \gamma\dot{\beta} \qquad \text{for } i = r, \theta, z \tag{34}$$

$$\dot{\varepsilon}_i^{\mathrm{tp}} = 3\kappa\dot{\beta}(1 - \beta)\sigma_i^{\mathrm{d}} \qquad \text{for } i = r, \theta, z \tag{35}$$

At this point, it is necessary to consider kinematics relations between strains and the radial displacement $u$ which is written as follows:

$$\varepsilon_r = \frac{\partial u}{\partial r}, \qquad \varepsilon_\theta = \frac{u}{r} \tag{36}$$

The three-dimensional equilibrium equations are reduced to

$$\frac{\partial \sigma_r}{\partial r} = \frac{\sigma_\theta - \sigma_r}{r} \tag{37}$$

Furthermore, the heat conduction problem is governed by the one-dimensional energy equation [**15**]

$$-\frac{\partial q}{\partial r} - \frac{1}{r}q = \rho c\dot{T} \tag{38}$$

and the constitutive relation between heat flux and temperature is established by the Fourier law

$$q = -\Lambda\frac{\partial T}{\partial r} \tag{39}$$

## 5 NUMERICAL PROCEDURE

The numerical procedure proposed here is based on the operator split technique [**8**, **12**] associated with an iterative numerical scheme in order to deal with non-linearities in the formulation. With this assumption, coupled governing equations are solved from the following four uncoupled problems:

1. *Thermal problem.* This consists of a radial conduction problem with surface convection. The material properties depend on temperature and, therefore, the problem is governed by non-linear parabolic equations. An implicit predictor–corrector procedure is used for numerical solution [**12**, **17**].
2. *Phase transformation problem.* The volumetric fraction of martensitic phase is determined in this problem. Evolution equations are integrated from a simple implicit Euler method [**17**, **18**].
3. *Thermoelastic problem.* The stress and displacement fields are evaluated from the temperature distribution. The numerical solution is obtained by employing a shooting method procedure [**17**, **18**].
4. *Elastoplastic problem.* Stress and strain fields are determined by considering the plastic strain evolution in the process. The numerical solution is based on the classical return mapping algorithm [**19**, **20**].

## 6 NUMERICAL SIMULATIONS

As an application of the general proposed model, numerical investigations of quenching of long steel cylindrical bar with radius $R = 22.5$ mm (SAE 4140H) are carried out, simulating a progressive induction (PI) hardening.

The material parameters of the cylinder are the following [1, 4]: $k = 1.100 \times 10^{-2}\ \text{K}^{-1}$, $\gamma = 1.110 \times 10^{-2}$, $\kappa = 5.200 \times 10^{-11}\ \text{Pa}^{-1}$, $\rho = 7.800 \times 10^3\ \text{kg/m}^3$, $M_s = 748$ K and $M_f = 573$ K. The other parameters depend on the temperature and need to be interpolated from experimental data. Therefore, the parameters $E$, $H$, $\sigma_Y$, $\alpha_T$, $c$, $K$ and $h$ are evaluated using the following expressions [21, 22]:

$$E = E_A(1-\beta) + E_M, \qquad \begin{cases} E_A = 1.985 \times 10^{11} - 4.462 \times 10^7 T - 9.909 \times 10^4 T^2 - 2.059 T^3 \\ E_M = 2.145 \times 10^{11} - 3.097 \times 10^7 T - 9.208 \times 10^4 T^2 - 2.797 T^3 \end{cases} \tag{40}$$

$$H = \begin{cases} 2.092 \times 10^6 + 3.833 \times 10^5 T - 3.459 \times 10^2 T^2, & \text{if } T \leqslant 723\ \text{K} \\ 2.259 \times 10^9 - 2.988 \times 10^6 T, & \text{if } 723\ \text{K} < T \leqslant 748\ \text{K} \\ 5.064 \times 10^7 - 3.492 \times 10^4 T, & \text{if } T > 748\ \text{K} \end{cases} \tag{41}$$

$$\sigma_Y = \begin{cases} 7.520 \times 10^8 + 2.370 \times 10^5 T - 5.995 \times 10^2 T^2, & \text{if } T \leqslant 723\ \text{K} \\ 1.598 \times 10^{10} - 2.126 \times 10^7 T, & \text{if } 723\ \text{K} < T \leqslant 748\ \text{K} \\ 1.595 \times 10^8 - 1.094 \times 10^5 T, & \text{if } T > 748\ \text{K} \end{cases} \tag{42}$$

$$\alpha_T = \begin{cases} 1.115 \times 10^{-5} + 1.918 \times 10^{-8} T - 8.798 \times 10^{-11} T^2 + 2.043 \times 10^{-13} T^3, & \text{if } T \leqslant 748\ \text{K} \\ 2.230 \times 10^{-5}, & \text{if } T > 748\ \text{K} \end{cases} \tag{43}$$

$$c = 2.159 \times 10^2 + 0.548 T \tag{44}$$

$$K = 5.223 + 1.318 \times 10^{-2} T \tag{45}$$

$$h = \begin{cases} 6.960 \times 10^2, & \text{if } T \leqslant 404\ \text{K} \\ 2.182 \times 10^4 - 1.030 \times 10^2 T + 1.256 \times 10^{-1} T^2, & \text{if } 404\ \text{K} < T \leqslant 504\ \text{K} \\ -2.593 \times 10^4 + 5.500 \times 10^2 T, & \text{if } 504\ \text{K} < T \leqslant 554\ \text{K} \\ -9.437 \times 10^4 + 4.715 \times 10^2 T - 7.286 \times 10^{-1} T^2 + 3.607 \times 10^{-4} T^3, & \text{if } 554\ \text{K} < T \leqslant 804\ \text{K} \\ 1.210 \times 10^3, & \text{if } T > 804\ \text{K} \end{cases} \tag{46}$$

PI hardening simulations consider a 5 mm thickness layer which is heated to 1120 K (850 °C) for 10 s and then immersed in a liquid medium at 293 K (20 °C) until a time instant of 120 s is reached. In order to consider the restriction associated with adjacent regions of the heated region, which is at lower temperatures, a plane strain state is adopted.

Reference [23] presents an experimental arrangement to promote PI hardening in cylindrical bodies. The experimental apparatus is depicted in Fig. 1. Figure 1a shows a schematic representation while Fig. 1b shows a photograph of the apparatus, which consists of a coil and a cooling ring. Experimental data obtained from this set-up are used here to validate the proposed model. Therefore, consider a cylindrical bar, which is quenched in the apparatus. Figure 2a shows a cross-section of a quenched bar submitted to a 2 per cent Nital etch, while Fig. 2b presents the Rockwell C hardness measurements. Using the X-ray diffraction peak technique [24], stress values on the surface layer were measured, giving $\sigma_\theta = -830$ MPa and $\sigma_z = -500$ MPa. These values show an uncertainty of 30 MPa.

Numerical simulations are considered in the forthcoming analysis. The temperature–time history for different positions of the cross-section is presented in Fig. 3. Note that, for regions with thickness greater than 5 mm ($r <$ 17.5 mm), the temperature does not reach the austenitizing limit.

The stress distribution over the radius for the final instant of time is shown in Fig. 4. Note that the stress values on the external surface are $\sigma_\theta = -866$ MPa and $\sigma_z = -255$ MPa. The circumferential stress $\sigma_\theta$ is close to experimental results. The longitudinal stress $\sigma_z$, on the other hand, has a discrepancy that could be explained by the assumption of a plane strain state adopted to simulate the restriction associated with adjacent regions of the heated region, which is at lower temperatures.

The analysis of phase transformation is now focused on. In order to compare numerical and experimental results, a relation between the volumetric fraction of the martensitic phase and the hardness is established. Therefore, it is assumed (Fig. 2b) that the martensitic phase ($\beta = 1$) has a Rockwell C hardness of 60 HRC while austenite ($\beta = 0$)

 

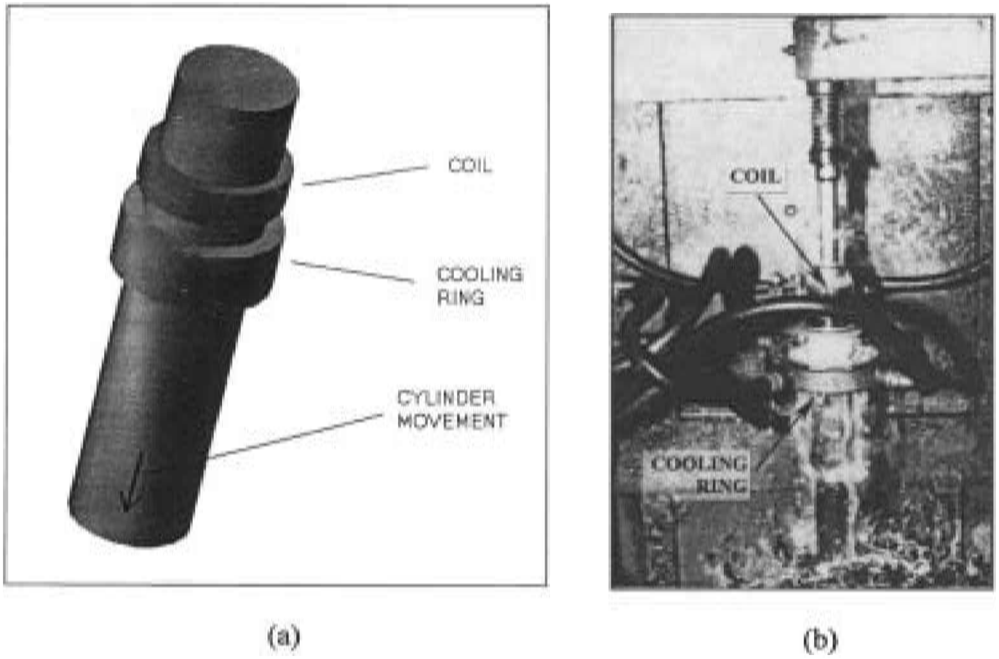


**Fig. 1** Experimental apparatus for PI hardening: (a) schematic view; (b) photograph of the experiment

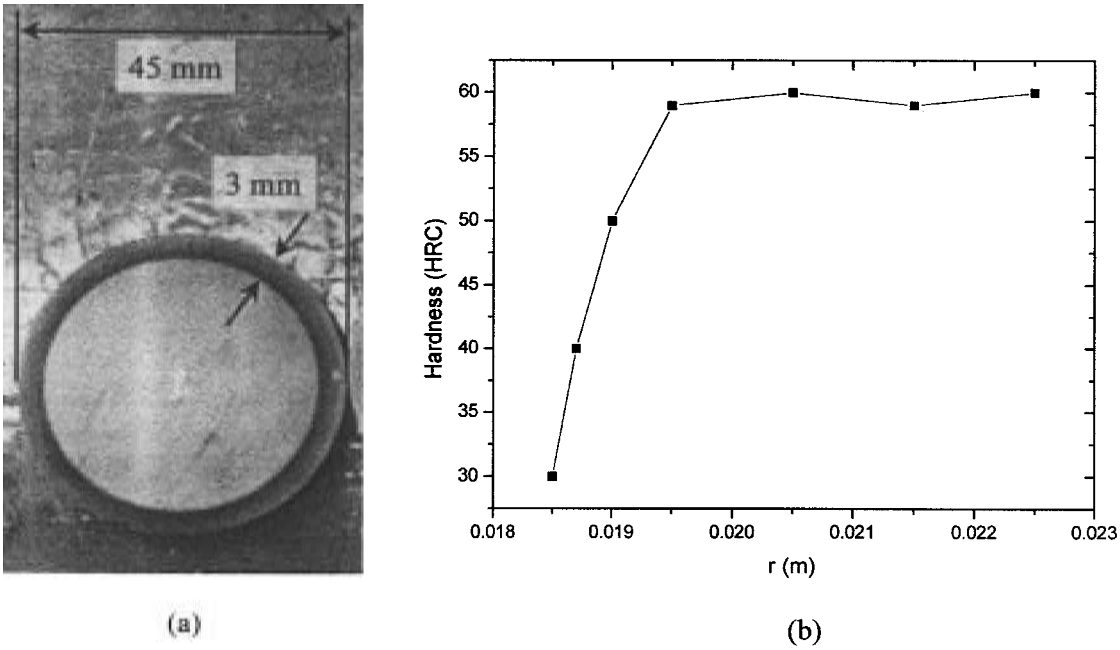


**Fig. 2** PI quenched body: (a) 2 per cent Nital etch of the cross-section view; (b) Rockwell C hardness measurements

has a Rockwell C hardness of 30 HRC. These represent typical values of martensitic and austenitic phases hardness [**22**, **23**]. Figure 5 presents both the volumetric fraction of martensite distribution, represented by variable $\beta$, and the experimental data related to the hardness measurements. Note that the process quenches only points from the external surface to a depth of 3 mm and, once again, the numerical results predicted by the model are close to the experimental data.

At this point, a comparison of the stress distributions for the final instant of time is made considering four different models, incorporating different effects: all transformation effects are considered (denoted TV&TP in Fig. 6); only volumetric transformation is considered (denoted TV in

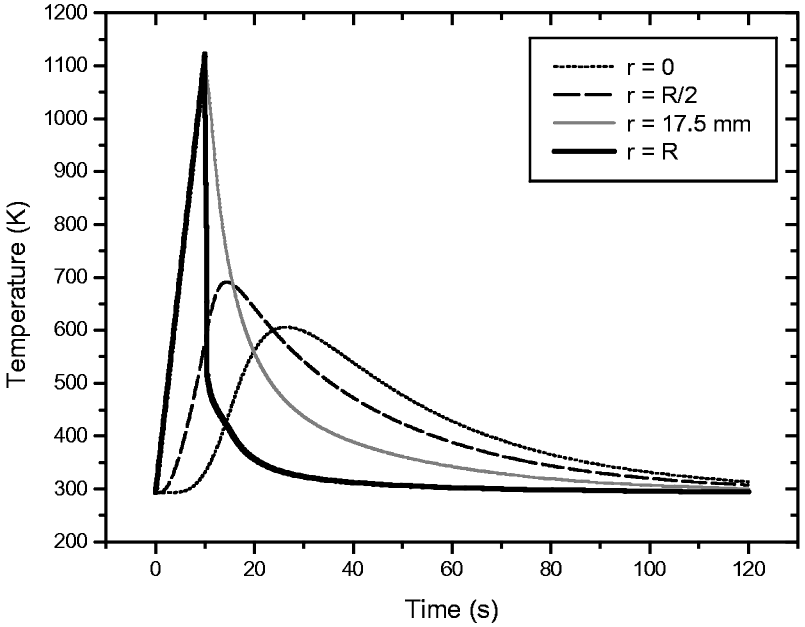


**Fig. 3** PI hardening: temperature–time history for different positions

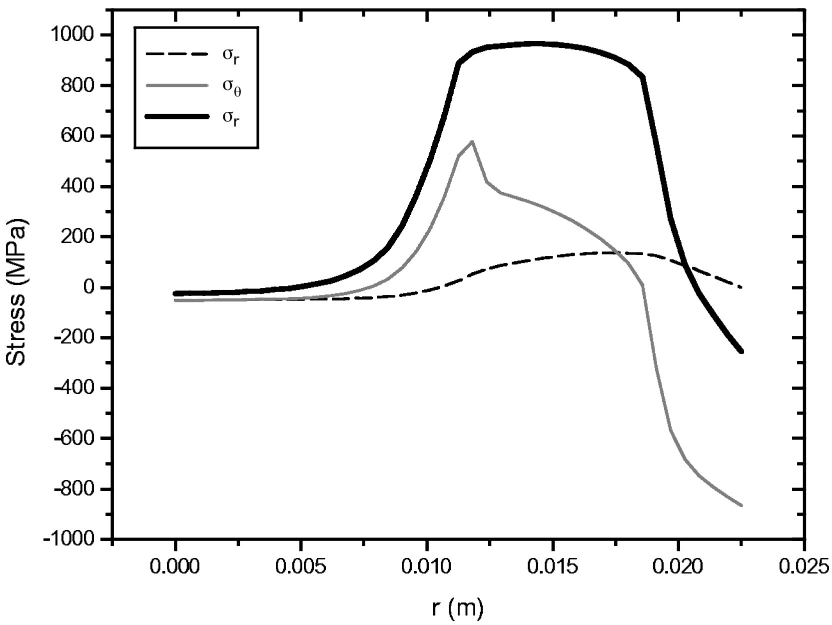


**Fig. 4** PI hardening: stress distribution for the final instant of time

Fig. 6); only transformation plasticity is considered (denoted TP in Fig. 6); no transformation effects are considered (denoted without TV&TP in Fig. 6). Figure 6 presents the stress distributions through the cross-section predicted by these four models. The results show that the general behaviour is qualitatively similar for the particular case study considered. However, a more detailed analysis, beyond the scope of this contribution, is necessary to elucidate the effect of these coupling terms in other situations.

## 7 CONCLUSIONS

The present contribution considers the modelling and simulation of the quenching process, presenting an anisothermal model formulated within the framework of continuum mechanics and the thermodynamics of irreversible processes. A numerical procedure is developed based on the operator split technique associated with an iterative numerical scheme in order to deal with nonlinearities in the formulation. PI hardening of a cylindrical

 

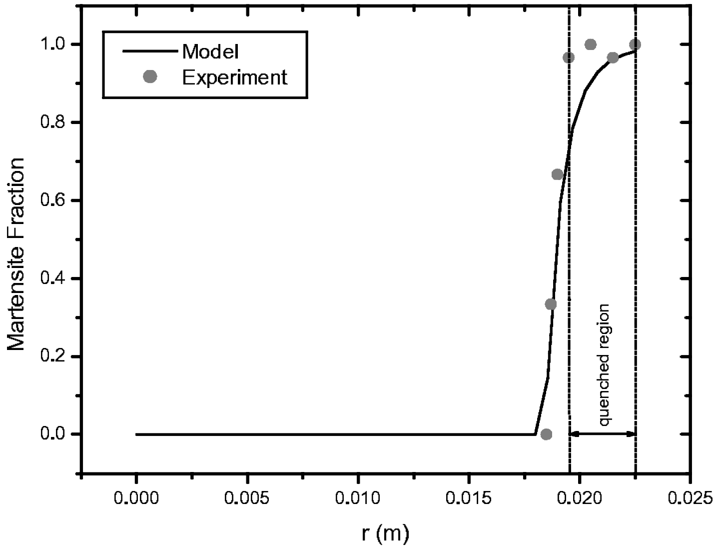


**Fig. 5** PI hardening: distribution of volume fraction of martensite for the final instant of time

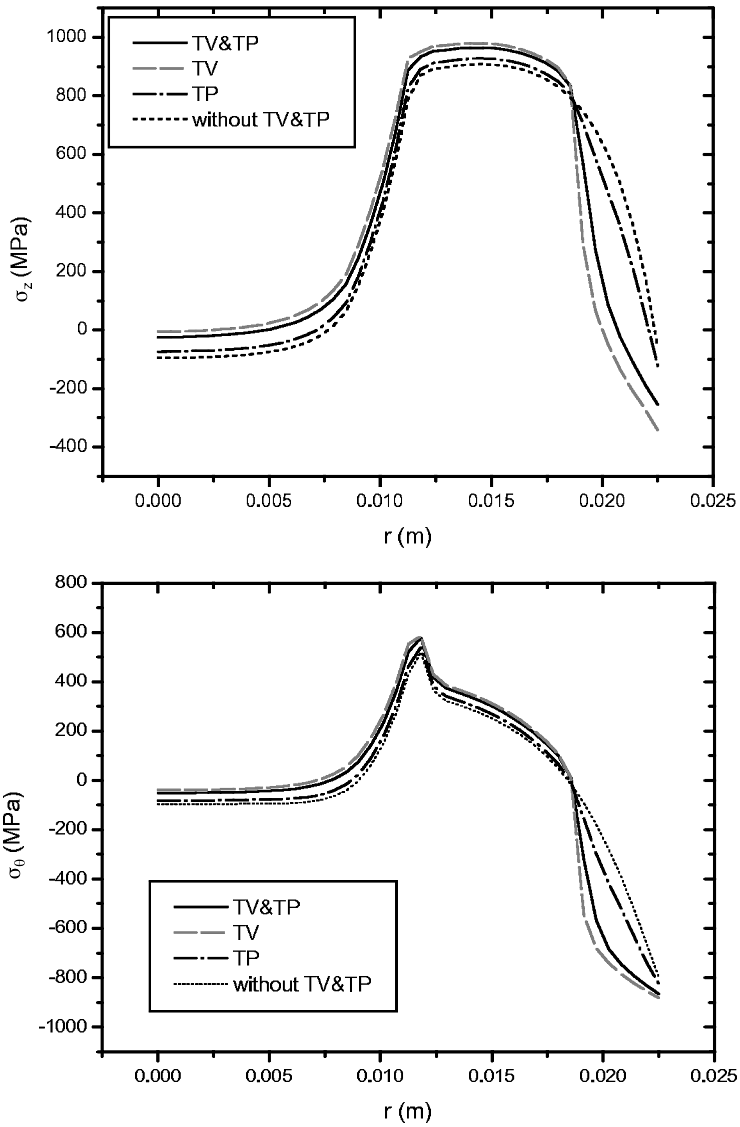


**Fig. 6** PI hardening: stress distributions for the final instant of time considering different transformation effects

body is considered as an application of the proposed general formulation. Numerical results suggest that the proposed model is capable of capturing the general behaviour of experimental data. An analysis of the stress distribution including different coupling terms shows that the general behaviour is qualitatively similar for the PI hardening of the cylindrical bar considered. The present authors agree that a more detailed analysis is necessary to elucidate the effect of these coupling terms in other situations.

## ACKNOWLEDGEMENTS

The authors would like to acknowledge the support of the Conselho Nacional de Desenvolvimento Científico e Tecnológico and the Fundação de Amparo a Pesquisa do Estado de Rio de Janeiro.

## REFERENCES

1 **Denis, S., Gautier, E., Simon, A.** and **Beck, G.** Stress–phase-transformation interactions—basic principles, modelling and calculation of internal stresses. *Mater. Sci. Technol.*, October 1985, **1**, 805–814.

2 **Denis, S., Archambault, S., Aubry, C., Mey, A., Louin, J. C.** and **Simon, A.** Modelling of phase transformation kinetics in steels and coupling with heat treatment residual stress predictions. *J. Physique IV*, September 1999, **9**, 323–332.

3 **Woodard, P. R., Chandrasekar, S.** and **Yang, H. T. Y.** Analysis of temperature and microstructure in the quenching of steel cylinders. *Metall. Mater. Trans. B*, August 1999, **4**, 815–822.

4 **Sjöström, S.** Interactions and constitutive models for calculating quench stresses in steel. *Mater. Sci. Technol.*, 1985, **1**, 823–829.

5 **Sen, S., Aksakal, B.** and **Ozel, A.** Transient and residual thermal stresses in quenched cylindrical bodies. *Int. J. Mech. Sci.*, 2000, **42**(10), 2013–2029.

6 **Eringen, A. C.** *Mechanics of Continua*, 1967 (John Wiley, New York).

7 **Lemaitre, J.** and **Chaboche, J.-L.** *Mechanics of Solid Materials*, 1990 (Cambridge University Press, Cambridge).

8 **Ortiz, M., Pinsky, P. M.** and **Taylor, R. L.** Operator split methods for the numerical solution of the elastoplastic dynamic problem. *Comput. Meth. Appl. Mechanics Engng*, 1983, **39**, 137–157.

9 **Desalos, Y., Giusti, J.** and **Gunsberg, F.** Deformations et contraintes lors du traitment thermique de pieces de acier. Report RE902, Institut de Recherches de la Sidérugie Française, 1982.

10 **Koistinen, D. P.** and **Marburger, R. E.** A general equation prescribing the extent of the austenite–martensite transformation in pure iron–carbon alloys and plain carbon steels. *Acta Metall.*, 1959, **7**, 59–60.

11 **Rockafellar, R. T.** *Convex Analysis*, 1970 (Princeton Press, Princeton, New Jersey).

12 **Pacheco, P. M. C. L.** Analysis of the thermomechanical coupling in elastoviscoplastic materials (in Portuguese). PhD thesis, Department of Mechanical Engineering, Pontifícia Universidade Católica do Rio de Janeiro, 1994.

13 **Pacheco, P. M. C. L., Oliveira, S. A., Camarão, A. F.** and **Savi, M. A.** A model to predict residual stresses introduced by the quenching process in steels (in Portuguese). In Proceedings of the XIV Brazilian Congress of Mechanical Engineering (*COBEM 97*), 1997.

14 **Camarão, A. F., da Silva, P. S. C. P.** and **Pacheco, P. M. C. L.** Finite element modeling of thermal and residual stresses induced by steel quenching (in Portuguese). In Seminário de *Fratura, Desgaste e Fadiga de Componentes Automobilísticos*, 2000 (Brazilian Society of Automotive Engineering, Rio de Janeiro).

15 **Boley, B. A.** and **Weiner, J. H.** *Theory of Thermal Stress*, 1985 (Krieger, Malabar, Florida).

16 **Chakrabarty, J.** *Theory of Plasticity*, 1987 (McGraw-Hill, New York).

17 **Ames, W. F.** *Numerical Methods for Partial Differential Equations*, 1992 (Academic Press, New York).

18 **Nakamura, S.** *Applied Numerical Methods in C*, 1993 (Prentice-Hall, Englewood Cliffs, New Jersey).

19 **Simo, J. C.** and **Miehe, C.** Associative coupled thermoplasticity at finite strains: formulation, numerical analysis and implementation. *Comput. Meth. Appl. Mechanics Engng*, 1992, **98**, 41–104.

20 **Simo, J. C.** and **Hughes, T. J. R.** *Computational Inelasticity*, 1998 (Springer-Verlag, Berlin).

21 **Melander, M.** A computational and experimental investigation of induction and laser hardening. PhD thesis, Department of Mechanical Engineering, Linkoping University, 1985.

22 **Hildenwall, B.** Prediction of the residual stresses created during quenching. PhD thesis, Linkoping University, 1979.

23 **Camarão, A. F.** A model to predict residual stresses in the progressive induced quenching of steel cylinders (in Portuguese). PhD thesis, Department of Metallurgical and Materials Engineering, Universidade de São Paulo, 1998.

24 Residual stress measurements by x-ray diffraction. SAE paper SAEJ 784A, 1980.

 